JOURNAL OF ENGINEERING SCIENCES

Volume 13, Issue 1 (2026)

Kozachenko O., Aliiev E., Dyakonov S., Pakhuchyi A., Volkovskii O., Luts P. (2026). Multi-criteria optimization of disk tillage implements with adjustable elastic shanks by substantiating design and operating parameters. Journal of Engineering Sciences (Ukraine), Vol. 13(1), pp. D14–D25. https://doi.org/10.21272/jes.2026.13(1).d2

p-ISSN 2312-2498
e-ISSN 2414-9381

Multi-Criteria Optimization of Disk Tillage Implements with Adjustable Elastic Shanks by Substantiating Design and Operating Parameters

Kozachenko O.[1][0000-0003-1326-4307], Aliiev E.[2*][0000-0003-4006-8803], Dyakonov S.[1][0000-0002-2451-5610], Pakhuchyi A.[1][0000-0002-7371-5264], Volkovskii O.[1][0009-0006-5516-0601], Luts P.[3][0000-0002-3776-8940]

[1] State Biotechnological University, 322/76, L. Pastera St., 63172, Kharkiv, Ukraine;
[2] Dnipro State Agrarian and Economic University, 25, S. Efremova St., 49000, Dnipro, Ukraine;
[3] Vinnytsia National Agrarian University, 3, Soniachna St., 21008, Vinnytsia, Ukraine

Article info:
Submitted: February 9, 2026
Received in revised form: April 20, 2026
Accepted for publication: April 23, 2026
Available online: April 27, 2026

***Corresponding author:**
aliev@meta.ua

Abstract. The research presents numerical and experimental investigations of a disk working element mounted on an elastic shank with a stiffness regulator. Using numerical simulation in SolidWorks, the distributions of stresses and deformations in the shank, their amplitude-frequency characteristics, and the influence of geometric parameters and disk orientation angles on system performance were determined. The analysis showed that the maximum absolute deformations at the disk attachment point and frame connection vary between 0.12 and 0.38 mm, while the maximum stresses in the shank and stiffness regulator range from 85 to 240 MPa, depending on design parameters. The optimal shank parameters ensured vibration stability in different directions and effective interaction between the disk and the soil, minimizing energy consumption and providing uniform surface tillage. Experimental tests conducted in a soil bin confirmed the patterns of variation in the draft force acting on the frame and on individual points of the shank, the vibration frequency of the working element, and soil compaction depending on the disk penetration depth, the travel speed of the implement, and the angle of the wedge-shaped insert. The results enabled the determination of rational operating parameters for the disk element that achieve an optimal balance between energy efficiency, stability of dynamic regimes, and soil tillage quality. The frame draft force varied in the range of 430–780 N, while local forces at the shank reached 310–690 N and 280–640 N, respectively. The vibration frequency of the working element was observed within 50–63 Hz. The results showed that the soil compaction coefficient ranged from 0.44 to 0.72, with a reduction of up to 39 % under optimal conditions. Overall, the proposed methodology combines numerical modeling with full-scale experiments, enabling comprehensive optimization of the design and technological characteristics of disk implements. The use of adjustable elastic shanks increases soil tillage efficiency, reduces draft resistance, and improves soil structure formation, making the proposed design suitable for modern resource-saving agricultural technologies.

Keywords: improved soil structure, draft force reduction, vibration stability, experimental study, numerical simulation.

1 Introduction

The intensification of agriculture, characteristic of most agrarian regions worldwide, has led to a significant increase in anthropogenic pressure on the soil cover, manifested in the degradation of soil structure, a decrease in humus content, compaction of the arable layer, and disruption of the soil water–air regime [1]. According to numerous studies [2, 3], traditional primary tillage systems involving soil inversion remain among the most energy-intensive and environmentally vulnerable technological operations in crop production, especially under conditions of climate change and soil moisture deficit.

In this regard, over the past two decades, a stable trend has been observed toward a transition from moldboard plowing to minimal and mulching tillage systems, the key element of which is the use of tillage implements with disk working bodies [4].

Disk implements provide a combination of shallow loosening, partial mixing of soil with crop residues, and reduced specific energy consumption, making them a fundamental tool of modern resource-saving technologies.

At the same time, despite significant progress in the structural development of disk tillage machines, many scientific publications [5–7] indicate the presence of unresolved problems related to instability of tillage depth, increased draft resistance, clogging of the inter-disk space, and insufficient adaptation of implements to variable soil and climatic conditions.

Of particular relevance is the optimization of the design and technological parameters of disk working bodies and their mounting shanks, which directly affect the quality and energy efficiency of surface tillage processes.

2 Literature Review

An analysis of scientific sources from recent decades indicates [8, 9] that disk tillage implements remain among the key technical means of surface soil tillage in modern crop production technologies. Studies [10, 11] devote considerable attention to improving the structural layouts of disk machines, optimizing operating parameters of working bodies, and investigating disk–soil interaction processes to enhance tillage quality and reduce energy consumption.

Simultaneously, the analysis of scientific publications indicates that most contemporary studies [12, 13] are fragmentary and focus mainly on individual aspects of the operation of disk working bodies. A significant number of publications are devoted to the experimental determination of the influence of disk geometric parameters (diameter, radius of curvature, angle of attack, and inclination angle) on soil tillage quality indicators and draft resistance [14–16]. These parameters are decisive in soil cutting, fragmentation, mixing, and crop residue chopping. However, in many studies [17, 18], these relationships are presented empirically and are not always supported by generalized theoretical models.

A separate group of studies is focused on improving the design of disk gangs and individual mounting systems for working bodies [19]. In modern technologies, a clear trend toward a transition from gang-based layouts to individual disk shanks is observed, driven by the need for better terrain following, improved stability of tillage depth, and reduced draft resistance. It has been proven that the use of elastic or spring-loaded shanks provides an additional benefit through the oscillatory motion of the working bodies, reducing resistance forces and improving soil structure disruption.

At the same time, critical analysis shows that most existing studies [20, 21] do not fully account for the complex stochastic nature of the interaction between disk working bodies and soil. In many studies, simplified models treat the soil medium as a homogeneous elastoplastic body, whereas real soil conditions are characterized by significant heterogeneity in physical and mechanical properties both with depth and across the field. This limits the practical applicability of the obtained results for predicting machine performance under various soil and climatic conditions.

An important direction of modern research is the application of numerical modeling methods (i.e., finite element and discrete element methods) to analyze the stress–strain state of soil and working bodies [22]. Such approaches allow a more detailed description of contact processes and force distribution; however, most publications lack sufficient experimental validation of the models. This necessitates combining numerical modeling with full-scale experimental testing.

Particular attention in recent studies [23, 24] is given to investigating the dynamic operating regimes of disk working bodies, including the influence of shank stiffness, working body mass, and implement travel speed on vibration amplitude and draft resistance. It has been established that optimizing elastic shank parameters can significantly reduce the energy consumption. However, in many studies, these issues are treated separately from disk geometric parameters, thereby preventing the development of comprehensive design recommendations for working bodies.

Notably, modern research pays insufficient attention to the mutual influence of disk and shank design parameters as a unified dynamic system “soil–disk–elastic element.” In most studies [25, 26], optimization is carried out for one or two parameters, whereas real operating conditions require a multi-factor approach. In addition, there is a practical lack of generalized optimization criteria that simultaneously account for soil tillage quality, process energy intensity, and structural reliability.

An analysis of publications [16–26] also shows that existing technical solutions for disk implements do not fully meet the requirements of modern resource-saving agricultural technologies. Despite the widespread adoption of disk machines with independent mounting of working bodies, ensuring stable tillage depth, reducing clogging by crop residues, and minimizing draft resistance remain relevant.

Thus, generalizing the results of contemporary research allows the conclusion that, despite significant scientific achievements in the field of disk tillage implements, some key issues remain insufficiently studied. These include comprehensive substantiation of the design and technological parameters of disk working bodies with elastic shanks, the development of adaptive designs with variable stiffness, and the creation of generalized mathematical models that adequately describe the dynamic interaction between implements and soil across a wide range of operating conditions.

The purpose of this research is to improve the operational efficiency of disk working bodies by substantiating the design and technological parameters of a disk harrow equipped with elastic shanks and a stiffness regulator.

To achieve this purpose, a scientific hypothesis was proposed, according to which improvements in soil tillage quality and reductions in energy consumption can be achieved by regulating and optimizing the elastic shank stiffness of a disk implement to adapt it to operating conditions.

The research objectives are as follows:

– to perform numerical modeling of the stress–strain state of the elastic shank of a disk harrow with a stiffness regulator and substantiate the ranges of its rational design parameters;

– to conduct experimental studies of the influence of design and operating parameters of the elastic shank of a disk tillage implement with a stiffness regulator on quality and energy performance indicators.

3 Research Methodology

3.1 Numerical simulation technique

A numerical study of the operation of a disk soil-tillage working body mounted on an elastic shank was conducted for the proposed design of a disk harrow (Figure 1), which consists of a frame and spherical disks mounted on individual elastic shanks of complex spatial geometry.

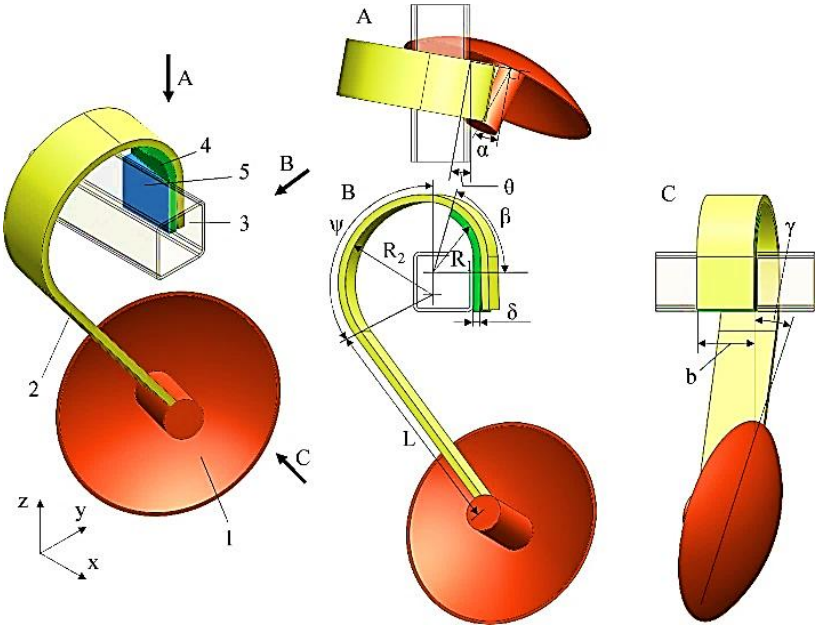

Figure 1 – Design of a disk soil-tillage working body mounted on an elastic shank

The shank design ensures the disk is installed at fixed angles of attack and inclination in the vertical–longitudinal plane, and allows stiffness adjustment via additional elastic plates and wedge-shaped inserts.

The interaction between the working body and the soil was considered a dynamic process, accompanied by periodic variations in the soil deformation resistance force. The total resistance of the soil medium was represented as the sum of a constant component, which accounts for friction, inertia, and disk penetration into the soil, and a variable component caused by soil deformation. The variable component of the deformation resistance force was assumed to vary according to a harmonic law, consistent with the data in [19]:

$$P_k = F_k \cos(\omega t + \gamma_k), \quad (1)$$

where P_k – the magnitude of the force in the direction of the k-th degree of freedom, N; ω – the excitation frequency, rad/s; t – time, s; γ_k – the phase angle of the force, rad.

The formulation of the numerical modeling problem is based on the analysis of forced vibrations of the nonlinear system "elastic shank – disk working body" under quasi-periodic loading. Projections of the soil resistance force, F_x, F_y, and F_z, were applied to the disk (Figure 2), determined using known empirical relationships as functions of the angle of attack, inclination angle, travel speed, and tillage depth, as well as the static load from the implement frame.

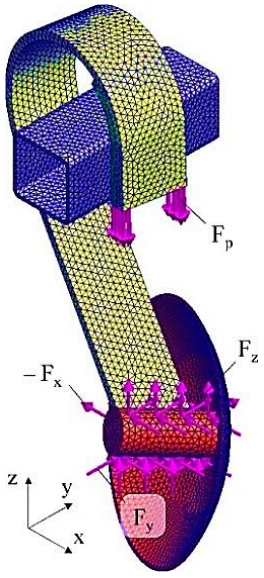

Figure 2 – Formulation of the numerical modeling problem

To evaluate the system's dynamic response, harmonic analysis was applied, enabling the determination of displacement, velocity, and acceleration amplitudes in the

steady-state regime under harmonic excitation. The equations of motion of the linear dynamic system were solved in modal form, including damping.

Since an analytical solution for a complex spatial structure is difficult, a numerical model was developed in SolidWorks 2023 SP 3.0 using linear dynamic analysis. The equations of motion were integrated using the Newmark method. For the computational model, a finite element mesh was generated with a characteristic element size of 1.9–21.2 mm and a growth factor of 1.4 (Figure 2).

The material of the shank and the stiffness regulator was assumed to be steel 60Si2A (Young's modulus – $2.12 \cdot 10^{11}$ N/m^2; Poisson's ratio – 0.29; shear modulus – $8.2 \cdot 10^{10}$ N/m^2; density – 7680 kg/m^3; ultimate tensile strength – $1.27 \cdot 10^9$ N/m²; yield strength – $1.09 \cdot 10^9$ N/m²), while the remaining elements were made of AISI 1035 steel (Young's modulus – $2.04 \cdot 10^{11}$ N/m^2; Poisson's ratio – 0.29; shear modulus – $7.99 \cdot 10^{10}$ N/m^2; density – 7850 kg/m^3; ultimate tensile strength – $5.85 \cdot 10^8$ N/m^2; yield strength – $2.82 \cdot 10^8$ N/m^2).

The calculations were performed with the following parameters: simulation duration – 10 s; number of analyzed frequencies – 15. The geometric parameters of the shank and the angular positions of the disk were set according to the base configuration, while the travel speed of the implement and the tillage depth were assumed to be constant.

As a result of numerical modeling, time-dependent distributions of stresses and deformations in the elastic shank were obtained. Zones of maximum stress were also identified. The features of the oscillatory process are presented in Figure 3.

Analysis of the amplitude–frequency characteristics (Figure 4) enabled determination of the natural frequencies of shank vibrations in the three Cartesian coordinate directions.

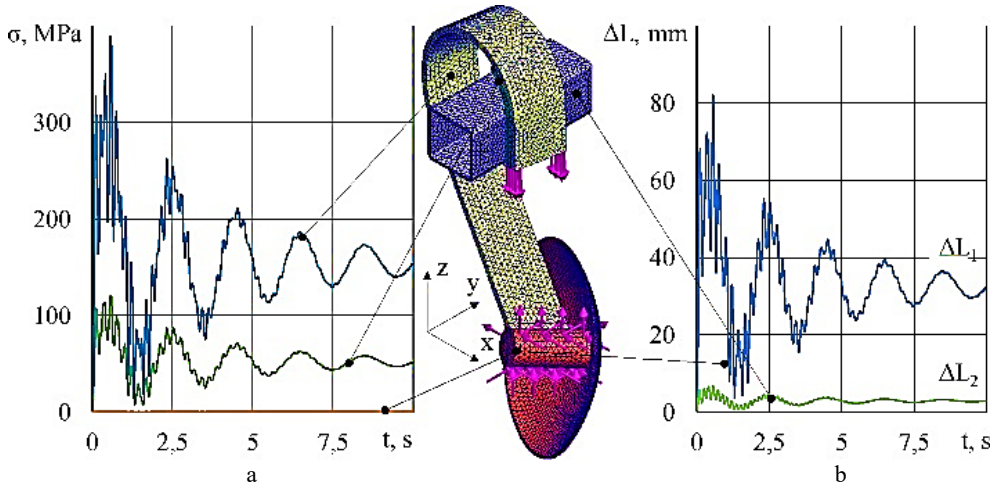

Figure 3 – Dynamics of changes at the shank bends: a – maximum stress σ, MPa; b – absolute deformation ΔL, mm

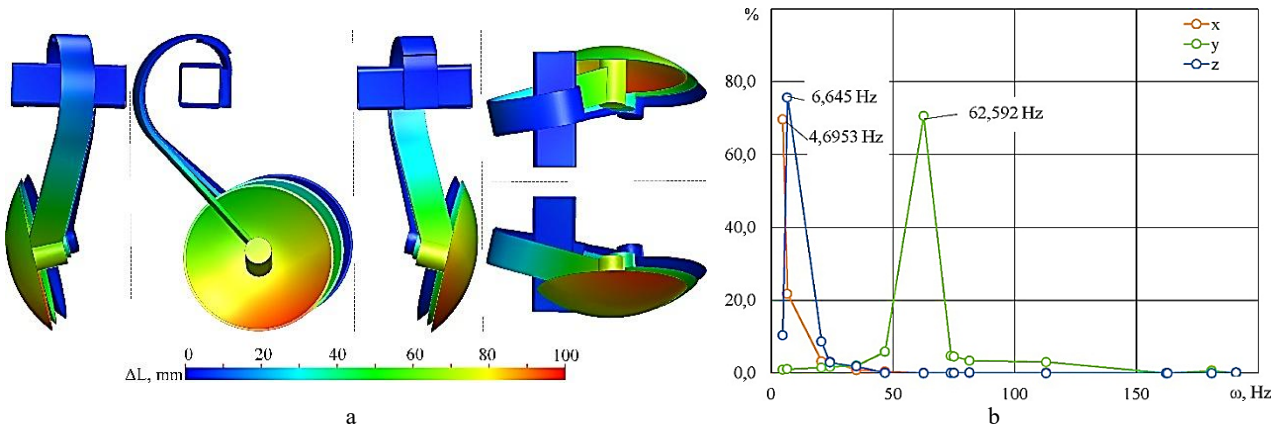

Figure 4 – Absolute deformations ΔL (a) and amplitude–frequency characteristics (b) of shank vibration

The conducted analysis of oscillations of the elastic shank of the disk harrow makes it possible to focus on the following evaluation criteria: the values of the maximum absolute deformation of the shank at the disk mounting point ΔL_1 and of the implement frame section ΔL_2; the maximum stress values at the bends of the shank and stiffness regulator σ_{R2} and σ_{R1}; and the natural vibration frequencies of the shank in three directions ω_x, ω_y, and ω_z.

Numerical simulations were performed in three stages:

1) the first stage with design parameters R_1 = 60–140 mm, R_2 120–200 mm, L = 300–500 mm, and ψ = 100–160°;

2) the second stage with design parameters $b = 80–130$ mm and $\delta = 8–16$ mm;

3) the third stage with design parameters $\gamma = 0–30°$, $\alpha = 0–30°$, $\theta = 0 \pm 10°$, and $\beta = 0–90°$.

The modeling was carried out according to a full factorial design with three-level factor coding. Processing of the results and construction of second-order regression equations were performed in the Wolfram Cloud, enabling the determination of optimal parameter values and the design of response surfaces.

3.2 Methodology of experimental research

Experimental studies of disk working bodies mounted on an elastic shank with a stiffness regulator were conducted in accordance with generally accepted methodologies for testing agricultural machinery under laboratory conditions. The tests were carried out in a soil bin with controlled motion regimes and adjustable tillage depth (Figure 5).

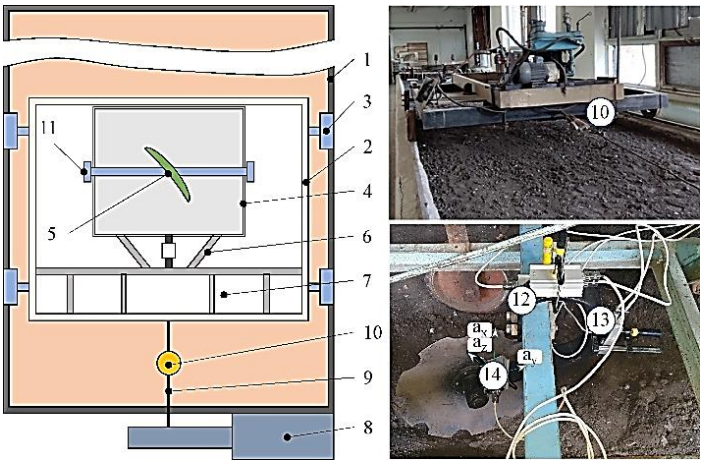

Figure 5 – Layout and general view of the soil bin with equipment for testing working bodies of soil-tillage machines: 1 – guide surface; 2 – frame; 3 – rollers; 4 – mounted movable frame; 5 – disk working bodies; 6 – mounting system; 7 – hydraulic mounting system; 8 – drive station; 9 – cable; 10 – frame draft force sensor (P_1, N); 11 – support wheel; 12 – strain gauge sensor on the shank (P_2, N); 13 – strain gauge sensor on the shank (P_3, N); 14 – inertial measurement unit

The investigated working bodies were mounted on the movable frame of the experimental setup, which moved along rail guides via a drive station with reversing capability. The travel speed of the setup was varied from 0.5 to 2.6 m/s, while the penetration depth of the disk working body was adjusted using a support wheel. Draft resistance was recorded using a strain gauge sensor. Before and during the experiments, the soil's physical and mechanical properties were determined.

The soil in the bin was pre-moistened, loosened, and compacted; soil moisture during the experiments ranged from 19 to 21 %. To ensure reliable results, the working section of the soil bin was divided into acceleration, measurement, and braking zones, and data acquisition was performed in the steady-state motion zone. Each test was repeated at least three times.

Measurements of draft force, travel speed, and dynamic parameters were carried out using a universal modular-type measuring system comprising a computing module, a sensor system, and an автономous power supply. The measuring system included strain gauge sensors for draft force measurement and an inertial measurement unit based on a three-axis accelerometer and gyroscope. Experimental data were processed and stored digitally, then analyzed.

Before testing, the strain gauge sensors were calibrated on a specialized test bench using a certified dynamometer. The calibration results showed a linear relationship between the applied force and the analog-to-digital converter output codes with a high coefficient of determination, confirming measurement accuracy.

Experimental investigations in the soil bin were conducted at three travel speeds, $v = 1.0$, 1.7, and 2.4 m/s. The penetration depth of the disk working body into the soil was 0.06, 0.10, and 0.14 m, respectively. Simultaneously, the angle of the wedge-shaped insert, θ, was varied over −6°, 0°, and 6°.

The following criteria were selected: the mean value of the force from the frame draft force sensor (P_1, N); the root mean square value of the force from the frame draft force sensor (σ_1, MPa); the vibration frequency of the working body (ω, rad/s); the mean force value from the upper shank force sensor (P_2, N); the mean force value from the extreme shank force sensor (P_3, N); the soil compaction coefficient K.

The soil compaction coefficient K is defined as the ratio of soil density after tillage to soil density before tillage:

$$K_h = \frac{\rho_h'}{\rho_h}, \quad (2)$$

where h – depth, m; ρ_h – the soil density before tillage, kg/m^3; ρ'_h – the soil density after tillage, kg/m^3.

The soil density was determined using an LAM-M density meter (penetrometer) at depths $h = 0.06$, 0.10, and 0.14 m.

To establish the patterns of influence of controlled factors on the performance indicators of the working body, a Box–Behnken design was used. Based on the

experimental results, second-order regression models were constructed in the Wolfram Cloud, and the significance of the coefficients and the adequacy of the models were verified using statistical criteria. The obtained mathematical models were used to determine rational operating parameters of the disk working body mounted on an elastic shank with a stiffness regulator.

4 Results

4.1 Numerical simulation results

As a result of numerical simulations performed in SolidWorks 2023 SP 3.0, data sets were generated for three research stages, each with determined study criteria.

To systematize the investigated factors, Table 1 presents the main parameters and their variation ranges used in the numerical experiments.

Table 1 – Main parameters and their variation ranges

Parameter	Description	Unit	Range of variation
R_1	Radius of upper shank bend	mm	60–140
R_2	Radius of lower shank bend	mm	120–200
L	Shank length	mm	300–500
b	Shank width	mm	80–130
δ	Shank thickness	mm	8–16
ψ	Shank inclination angle	°	100–160
α	Disk attack angle	°	0–30
β	Disk tilt angle	°	0–90
γ	Disk rotation angle	°	0–30
θ	Additional inclination angle	°	0 ± 10

For the first stage of the study, the following design parameters were adopted: $b = 100$ mm, $\delta = 14$ mm, $\alpha = 15°$, $\gamma = 15°$, $\beta = 90°$, and $\theta = -5°$.

Processing of the obtained data yielded the following relationships (Figure 6):

$$\Delta L_1 = -1233.7 + 2.13L - 0.00219L^2 + \\ +5.55\,\psi - 0.02714\,\psi^2 + 1.103\,R_1 - 0.0116R_1^2 + \\ + 8.968R_2 - 0.0261R_2^2; \quad (3)$$

$$\Delta L_2 = 54.93 - 0.0944L + 0.00014L^2 - 0.487\psi + \\ +0.00159\,\psi^2 - 0.4515\,R_1 + 0.00164\,R_1^2 + \\ +0.3724\,R^2 - 0.000983\,R_2^2; \quad (4)$$

$$\sigma_{R1} = -15.03 + 0.0202\,L - 0.0000238L^2 + \\ +0.068\psi - 0.000235\psi^2 + 0.00608\,R_1 - \\ -0.000114R_1^2 + 0.1272R_2 - 0.000428R_2^2; \quad (5)$$

$$\sigma_{R2} = 1047.02 - 1.312\,L + 0.0017L^2 - \\ -7.18869\,\psi + 0.0311\psi^2 - 6.688R_1 + \\ +0.02257R_1^2 + 2.777R_2 - 0.01075R_2^2. \quad (6)$$

The calculated Fisher criteria ($F_{\Delta L1} = 65266$, $F_{\Delta L2} = 65266$, $F_{\sigma R1} = 6934$, and $F_{\sigma R2} = 36915$) significantly exceed the tabulated value $F_{0.05}(15, 66) = 1.84$, indicating the statistical significance and adequacy of the developed regression models.

To ensure optimal operating conditions of the elastic shank, it is necessary to achieve the maximum deformation of the shank at the disk mounting point (ΔL_1) while minimizing the deformation of the implement frame (ΔL_2):

$$\Delta L_1 \to max;\ \Delta L_2 \to min. \quad (7)$$

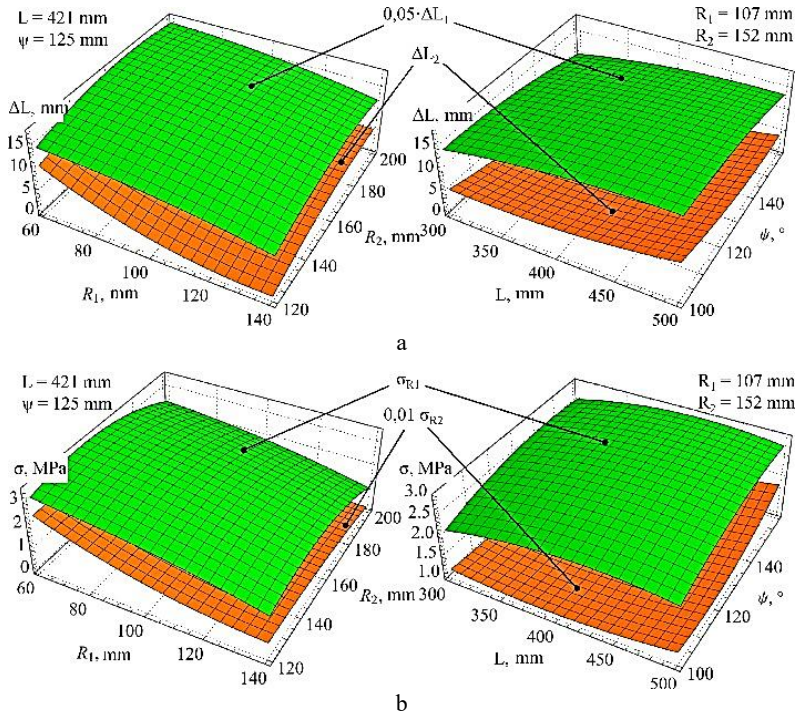

Figure 6 – Dependencies of the maximum absolute deformation of the shank at the disk mounting point ΔL_1 and deformation of the implement frame section ΔL_2 (a), as well as maximum stresses at the shank bends and stiffness regulator σ_{R1}, σ_{R2} (b) on the research factors R_1, R_2, L, and ψ

After scalar ranking, the compromise problem (3) can be solved by maximizing the multiplicative objective function:

$$M = \frac{\Delta L_1 - min(\Delta L_1)}{max(\Delta L_1) - min(\Delta L_1)} \cdot \frac{max(\Delta L_2) - \Delta L_2}{max(\Delta L_2) - min(\Delta L_2)} \rightarrow max. \quad (8)$$

Solving equation (8) jointly with equations (3) and (4) using the Wolfram Cloud software yielded rational geometric parameters of the disk harrow shank: R_1 = 106 mm, R_2 = 151 mm, L = 420 mm, and ψ = 125°.

For these parameters, the stress values were σ_{R1} = 2.88 MPa and σ_{R2} = 99.95 MPa. At the first stage of the study, the natural vibration frequencies of the shank in three directions were ω_x = 4.61 ± 0.21 Hz, ω_y = 62.68 ± 1.98 Hz, and ω_z = 6.65 ± 0.28 Hz.

For the second stage, the following design parameters were adopted: R_1 = 106 mm, R_2 = 151 mm, L = 420 mm, ψ = 125°, γ = 15°, α = 15°, θ = –5°, and β = 90°.

As a result of data processing, the following relationships were obtained (Figure 7):

$$\Delta L_1 = -175.64 - 0.0215b^2 + b(2.295 - 0.0196\delta) + \\ +43.802\delta - 1.565\delta^2; \quad (9)$$

$$\Delta L_2 = 35.49 - 0.0249b - 0.00222b^2 + \\ +0.9307\delta - 0.0387\delta^2; \quad (10)$$

$$\sigma_{R1} = 8.59 - b(0.0394 + 0.000344\delta) + \\ +0.03064\delta - 0.00275\delta^2; \quad (11)$$

$$\sigma_{R2} = 240.76 - 1.9461b + \\ +0.00632b^2 - 1.9408\delta. \quad (12)$$

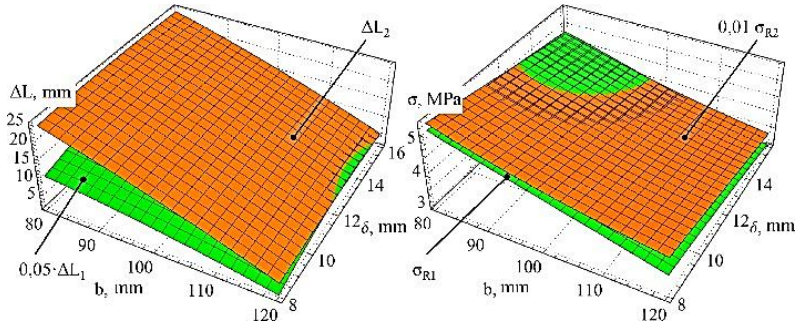

Figure 7 – Dependencies of the maximum absolute deformation of the shank at the disk attachment point ΔL_1 and the implement frame ΔL_2 (a), as well as the maximum stresses at the bends of the shank and stiffness regulator σ_{R1}, σ_{R2} (b) on the study factors b and δ

The calculated Fisher criteria ($F_{\Delta L1}$ = 21062, $F_{\Delta L2}$ = 7802, $F_{\sigma R1}$ = 57346, and $F_{\sigma R2}$ = 205290) exceed the tabulated value $F_{0.05}(6, 3)$ = 8.94, confirming the adequacy of the regression models.

Solving equation (8) jointly with equations (9) and (10) yielded rational geometric parameters of the shank: b = 109 mm and δ = 14 mm.

For these parameters, the stress values were σ_{R1} = 3.65 MPa and σ_{R2} = 76.96 MPa.

At the second stage, the natural vibration frequencies were ω_x = 4.63 ± 0.26 Hz, ω_y = 60.43 ± 1.61 Hz, and ωz = 6.69 ± 0.20 Hz.

For the third stage, the following parameters were adopted: R_1 = 106 mm, R_2 = 151 mm, L = 420 mm, ψ = 125°, b = 109 mm, and δ = 14 mm.

The following relationships were obtained (Figure 8):

$$\Delta L_1 = -66.7 - 0.02975\,\alpha^2 - 0.05988\,\beta^2 + \\ +\beta\,(3.1945 - 0.03951\,\theta) + \alpha(1.268 + \\ +0.03675\,\theta) + 1.456\,\theta - 0.0608\,\theta^2; \quad (13)$$

$$\Delta L_2 = 3.755 + 0.00545\alpha - 0.0044\beta + 0.0132\,\theta; \quad (14)$$

$$\sigma_{R1} = 0.7146 + 0.00659\,\alpha - 0.000024954\,\beta^2 + \\ +\beta\,(0.00365 + 0.000034560) + \\ +0.01447\theta + 0.0007031\theta^2; \quad (15)$$

$$\sigma_{R2} = 86.8175 + 1.0148\alpha + 0.3018\beta + 1.711\theta. \quad (16)$$

The calculated Fisher criteria ($F_{\Delta L1}$ = 11567, $F_{\Delta L2}$ = 1713, $F_{\sigma R1}$ = 1267, and $F_{\sigma R2}$ = 16837) exceed the tabulated value $F_{0.05}(15, 66)$ = 1.84, confirming the adequacy of the models.

Solving equation (8) jointly with equations (13) and (14) yielded rational shank parameters: α = 9.7°, γ = 15°, β = 48.8°, and θ = 5.2°.

For these parameters, the stresses were σ_{R1} = 0.82 MPa and σ_{R2} = 100.28 MPa.

At the third stage, the natural vibration frequencies were: ω_x = 4.25 ± 0.21 Hz, ω_y = 61.29 ± 2.57 Hz, and ω_z = 6.66 ± 0.11 Hz.

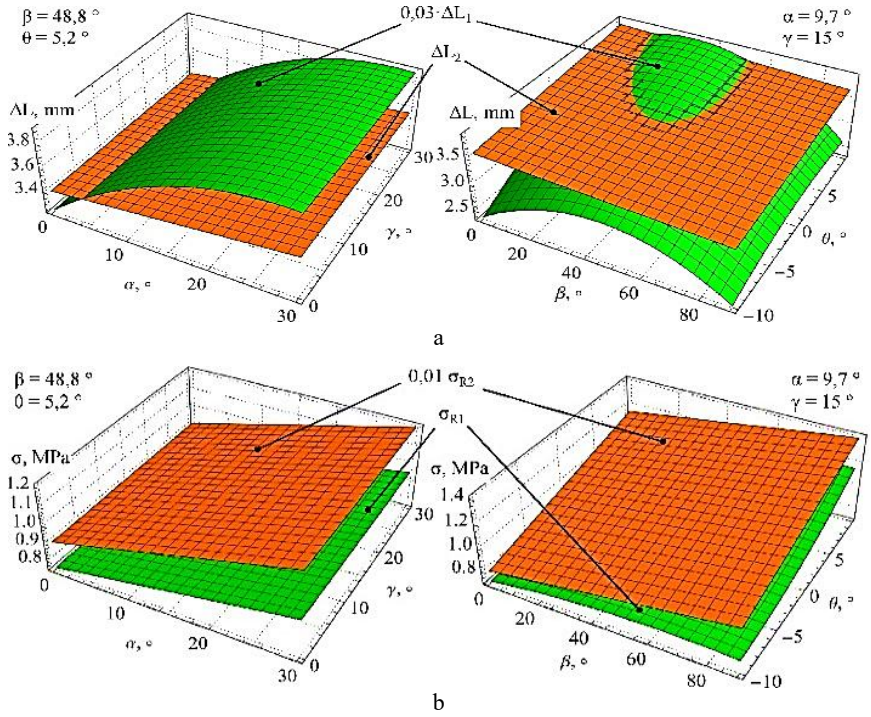

Figure 8 – Dependencies of the maximum absolute deformation of the shank at the disk attachment point ΔL_1 and the implement frame section ΔL_2 (a), as well as the maximum stresses on the shank and stiffness regulator σ_{R1}, σ_{R2} (b) on the research factors α, β, γ, and θ

4.2 Results of experimental studies

As a result of the experimental studies, dependencies of the dynamics of the frame traction force P_1 and the traction forces at the upper and extreme points of the shank (P_2 and P_3) were obtained for each trial. Examples of these dependencies are shown in Figure 9.

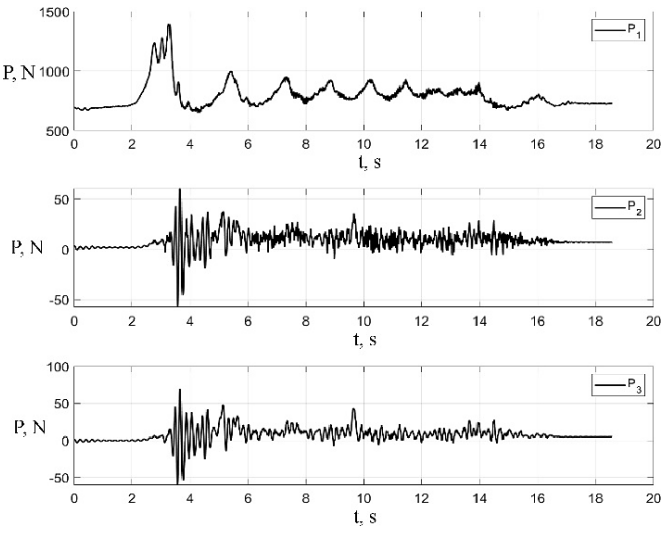

Figure 9 – Dependencies of the dynamics of traction forces P_1, P_2, and P_3 at v = 1.0 m/s, h = 0.06 m, and θ = 0°

The graphs in Figure 9 show fluctuations in the traction forces, confirming the disk's oscillatory behavior on the elastic shank. After calculating the mean values, root-mean-square deviations, and oscillation frequencies, a dataset of generalized results was compiled.

From the data processing, the following relationships were obtained (Figure 10):

$$P_1 = 19.9583 + 400.1\,h + \\ +19.75\,V - 2.8625\,\theta - 0.560185\,\theta^2; \quad (17)$$

$$P_2 = -15.1143 + 617.5\,h + \\ +16.2143\,V - 1.8625\,\theta - 0.222917\,\theta^2; \quad (18)$$

$$P_3 = -12.5247 + 350.313\,h + \\ +8.83929\,V - 0.933333\,\theta - 0.0945602\,\theta^2; \quad (19)$$

$$\omega = 39.36 + 76.87\,h + 10.37V - \\ -2.568V^2 - 0.2458\,\theta + 0.0678\,\theta^2. \quad (20)$$

The calculated Fisher criteria (F_{P1} = 699.45, F_{P2} = 776.2, F_{P3} = 741.4, and F_{ω} = 3690.5) are significantly higher than the tabulated value $F_{0.05}(10, 5)$ = 4.74, indicating the statistical significance and adequacy of the constructed regression models.

Using the Wolfram Cloud, a regression equation was formed to determine the soil compaction coefficient (Figure 11):

$$K = 0.5166 + 0.1384h - 0.02678V + \\ +0.8928hV + 0.0188\,\theta. \quad (21)$$

The calculated Fisher criterion F_K = 1050 is significantly higher than the tabulated value $F_{0.05}(10, 5)$ = 4.74, confirming the regression model's statistical significance and adequacy.

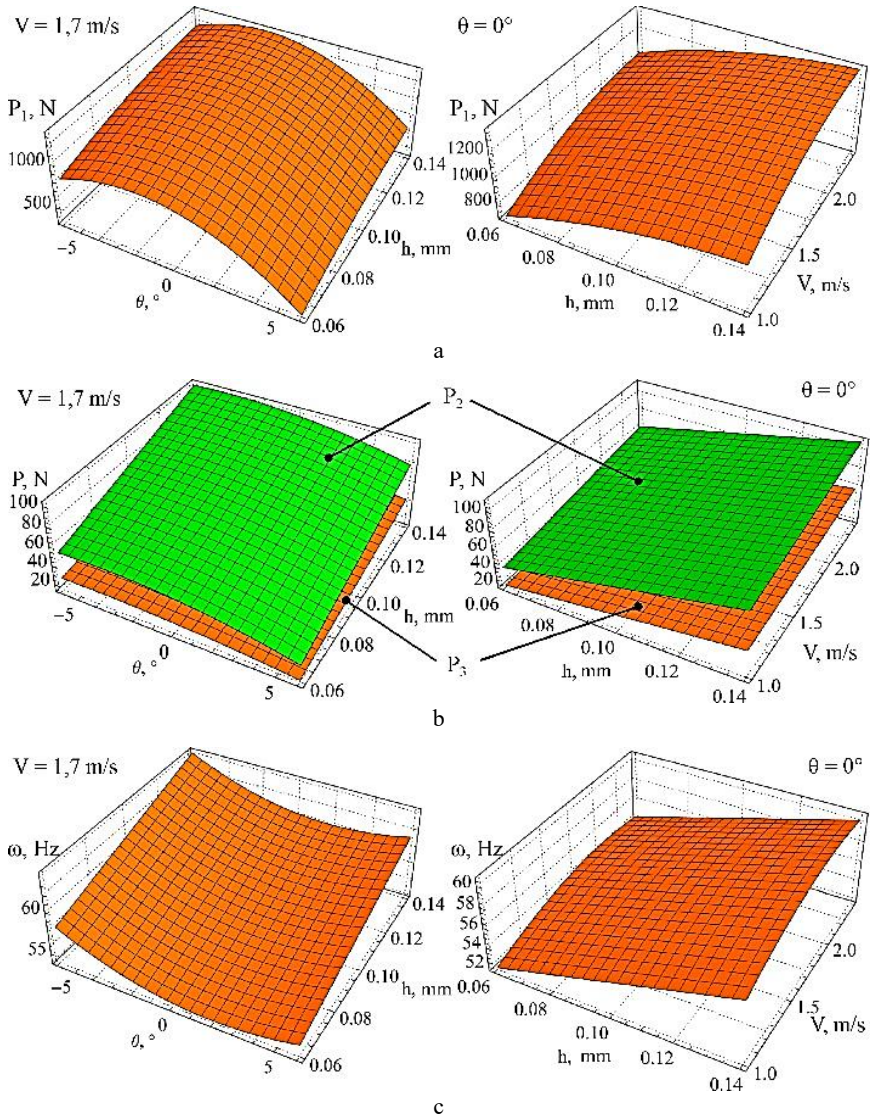

Figure 10 – Dependencies of the mean traction force from the frame sensor P_1 (a), at the upper P_2 and extreme P_3 points (b) of the shank, as well as the working body oscillation frequency ω (c) on the study factors θ, h, and v

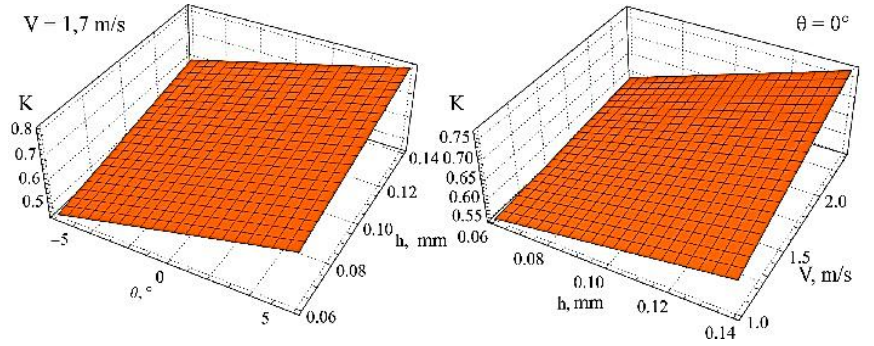

Figure 11 – Dependencies of the soil compaction coefficient K on the study factors θ, h, and v

Analysis of optimal factor values based on minimizing the mean frame traction force P_1, the working body oscillation frequency ω, and the soil compaction coefficient K showed that the disk shank wedge insertion angle θ does not have a clear optimal value. In contrast, the penetration depth $h = 0.06$ m and the travel speed $v = 1.0$ m/s were determined as rational. This is explained by the fact that changing the angle θ affects all criteria differently: increasing the angle may reduce traction resistance but simultaneously increase the compaction coefficient, or vice versa. Therefore, a compromise solution is required to reconcile the influence of all factors and determine such a value of θ that ensures an acceptable level of energy consumption and agronomic performance.

The problem is formulated as a multi-criteria optimization and reduces to solving the system of equations:

$$\begin{cases} P_1(\theta, h, L) \to min; \\ \omega(\theta, h, L) \to min; \\ K(\theta, h, L) \to min. \end{cases} \quad (22)$$

The ranking method is applied to solve multi-criteria problems when it is necessary to choose a compromise solution among several alternative values of a parameter, taking into account different optimization criteria. To select a compromise θ value, a set of alternative parameter values is formed, and the criteria are calculated for each. Since the indicators have different units and ranges, they are normalized, usually by the min–max method, which converts all criteria to a single scale ("the higher, the better") if all are to be minimized. Next, weight coefficients reflecting the relative importance of each criterion (i.e., energy efficiency, dynamic stability, or agronomic quality) are assigned. Then, for each alternative, an integral score is calculated as the weighted sum of the normalized values of all criteria. The resulting integral scores allow ranking the alternatives and determining the θ value that provides the best compromise among all criteria. If several alternatives yield close results, additional analysis is conducted, e.g., by checking solution stability under weight changes or by refining results experimentally.

Thus, the ranking method formalizes the decision-making process and selects the optimal design parameter value in the presence of several conflicting criteria:

$$\frac{P_1(\theta,h,L)-P_{1min}}{P_{1max}-P_{1min}} \cdot \frac{\omega(\theta,h,L)-\omega_{min}}{\omega_{max}-\omega_{min}} \cdot \frac{K(\theta,h,L)-K_{min}}{K_{max}-K_{min}} \to min. \quad (23)$$

Solving equation (23) in Wolfram Cloud yielded the following results: θ = 2.32°, h = 0.06 m, and v = 1.0 m/s. In this case, P_1 = 543 N, ω = 51.6 Hz, and K = 0.59.

5 Discussion

The results of numerical modeling and experimental studies confirm that the design and technological parameters of the elastic shank of a disk working body significantly affect oscillation dynamics, traction resistance, and soil compaction. In particular, the optimal values of the shank's geometric parameters and disk installation angles allow for maximum deformation at the disk attachment point while minimizing stresses in the frame, which aligns with current trends in the use of individual elastic shanks [19, 25, 26].

Similar findings were observed in study [14], which emphasized the role of the disk's attack and tilt angles on soil cultivation quality and traction resistance, although most of these works did not consider the combined effect of the shank and disk parameters as a single system.

Experimental data confirm that the penetration depth of the disk and the travel speed of the implement are critical factors affecting the traction force and oscillations of the working body, consistent with conclusions in [15, 16], which also noted that insufficient adaptation of implements to variable soil-climatic conditions leads to unstable operation and increased energy consumption.

Simultaneously, the obtained regression models allow evaluation of the effect of the adjustment wedge angle θ on all performance indicators, providing a multi-criteria compromise – a novel approach compared to most previous works, which considered only individual factors [17, 18, 20].

The results also confirm that using elastic shanks with a stiffness regulator significantly reduces the oscillation amplitude of the working body in the *Ox* and *Oz* directions, while simultaneously ensuring stable operation along *Oy*. This aligns with findings in [25, 26] regarding the positive effect of oscillatory motion on reducing resistance forces and improving soil structure disruption.

Simultaneously, compared with studies [21, 22], the results allow for the quantitative determination of rational shank and disk parameters for multi-factor optimization, which is important for practical application in resource-saving agricultural technologies.

Thus, the conducted study confirms the effectiveness of an integrated approach combining numerical modeling and field testing, enabling generalized recommendations on the design and technological parameters of disk working bodies that achieve an optimal balance between energy efficiency, dynamic stability, and soil cultivation quality.

6 Conclusions

Based on numerical modeling in SolidWorks, the temporal distributions of absolute deformation and stress for the disk harrow shank, as well as its amplitude-frequency vibration characteristics, were visualized.

Processing of the obtained data made it possible to establish dependencies of the maximum absolute deformation of the shank at the disk attachment point and at the implement frame section, as well as the maximum stresses on the shank and the stiffness regulator, on the geometric dimensions of the shank (including the radii of curvature, its length, the bend angle, width, and thickness), and on the spatial orientation parameters of the disk (attack angle, tilt angle), the adjustment plate angle, and the second bend angle of the shank.

The rational geometric parameters of the disk harrow shank were determined as follows: the radius of the first bend is 106 mm, the radius of the second bend is 151 mm, the shank length is 420 mm, the main bend angle is 125°, the shank width is 109 mm, and the thickness is 14 mm. The rational spatial placement parameters are: the disk attack angle is 9.7°, the disk tilt angle is 15°, the inclination angle relative to the direction of motion is 48.8°, and the adjustment plate angle is 5.2°.

For each spatial direction, a maximum vibration amplitude was observed. In the longitudinal direction, this corresponds to the first mode at 4.25 ± 0.21 Hz; in the transverse direction, to the second mode at 61.29 ± 2.57 Hz; and in the vertical direction, to the third mode at 6.66 ± 0.11 Hz. Changes in the shank design parameters did not significantly affect these modes and

frequencies, which remained within the statistical error range.

Experimental studies made it possible to determine the dynamics of the traction force of the implement frame, as well as the traction forces at the upper and extreme points of the disk working body shank, for each test according to a three-factor Box–Behnken experimental design (including the wedge angle of the shank, the depth of penetration, and the travel speed at three levels of variation).

Processing of the experimental data using Wolfram Cloud resulted in second-order regression equations for the average frame traction force, its root mean square deviation, the vibration frequency of the working body, and the average forces at the upper and extreme points of the shank as functions of the wedge angle, penetration depth, and travel speed.

The combined results of experimental research and mathematical modeling show that the soil compaction coefficient is primarily determined by the combination of the disk working body's depth of penetration and travel speed, while the shank's wedge angle has a secondary effect. Increasing the depth and speed leads to more intensive soil compaction due to the larger volume of displaced soil and intensified crumbling processes, consistent with the physical principles governing the interaction between the working body and the soil.

Optimizing the regression equations allowed determining the parameters that minimize soil compaction: the wedge angle is –6°, the penetration depth is 0.06 m, and the travel speed is 1.0 m/s, yielding a minimum compaction coefficient of 0.44.

Optimization of the design and technological parameters showed that rational values of the penetration depth of 0.06 m and travel speed of 1.0 m/s provide a balance between energy consumption and agronomic efficiency, while the wedge angle should be determined through a compromise. Using a ranking method yielded an optimal wedge angle of 2.32°, ensuring acceptable levels of frame traction force (543 N), working body vibration frequency (51.6 Hz), and soil compaction coefficient (0.59).

These results demonstrate the effectiveness of multi-criteria optimization for improving the quality and energy efficiency of disk harrow operation.

Further research should focus on several directions. First, the application of the discrete element method (DEM) is planned to provide a more detailed representation of soil–tool interaction at the particle level and to compare DEM-based results with the obtained experimental and numerical data.

Second, it is advisable to extend the study to different soil types, moisture contents, and residue conditions to validate the robustness of the proposed design and operating parameters across varying field conditions. Third, future work will consider the coupled use of finite element and discrete element approaches to account for structural dynamics and soil behavior simultaneously. In addition, investigation of long-term durability and fatigue strength of the elastic shank under cyclic loading is required.

Finally, integrating sensor-based monitoring with precision agriculture practices will enable real-time adaptive control of operating parameters, further improving energy efficiency and soil conservation outcomes.

References

1. Sartori, F., Piccoli, I., Polese, R., Berti, A. (2022). Transition to conservation agriculture: how tillage intensity and covering affect soil physical parameters. *Soil*, Vol. 8, pp. 213–222. https://doi.org/10.5194/soil-8-213-2022
2. Lv, L., Gao, Z., Liao, K., Zhu, Q., Zhu, J. (2023). Impact of conservation tillage on the distribution of soil nutrients with depth. *Soil and Tillage Research*, Vol. 225, 105527. https://doi.org/10.1016/j.still.2022.105527
3. Negrete-Rodríguez, M.L.X., Conde-Barajas, E., Silva-Martínez, G.A., Acosta-García, G., Ramírez-Medina, H., Tristán-Flores, F.E., Bedolla-Rivera, H.I. (2024). Tillage and its effect on agricultural soils: A quality index approach. *Agronomy*, Vol. 14(12), 2793. https://doi.org/10.3390/agronomy14122793
4. Winkler, J., Dvořák, J., Hosa, J., Barroso, P.M., Vaverková, M.D. (2023). Impact of conservation tillage technologies on the biological relevance of weeds. *Land*, Vol. 12(1), 121. https://doi.org/10.3390/land12010121
5. Novara, A., Novara, A., Comparetti, A., Santoro, A., Cerdà, A., Rodrigo-Comino, J., Gristina, L. (2022). Effect of standard disk plough on soil translocation in sloping Sicilian vineyards. *Land*, Vol. 11(2), 148. https://doi.org/10.3390/land11020148
6. Munteanu, C., Tufescu, A., Lupu, F.C., Istrate, B., Benchea, M., Melnic, I., Vișanu, V., Arsenoaia, V.N. (2026). Explicit FEM analysis of soil–disc interaction for APS-coated notched harrow discs in representative agricultural soils. *Applied Sciences*, Vol. 16(1), 395. https://doi.org/10.3390/app16010395
7. Hrushetskyi, S., Bodnaruk, B. (2024). Model of analytical study of the interaction of the disc working body with the soil. *International Science Journal of Engineering & Agriculture*, Vol. 3(5), pp. 30–43. https://doi.org/10.46299/j.isjea.20240305.04
8. Zhong, G., Li, H., He, J., Wang, Q., Lu, C., Wang, C., Tong, Z., Cui, D., He, D. (2023). Design and test of single-disc opener for no-till planter based on support cutting. *Agriculture*, Vol. 13(8), 1635. https://doi.org/10.3390/agriculture13081635
9. Zeng, Z., Thoms, D., Chen, Y., Ma X. (2021). Comparison of soil and corn residue cutting performance of different discs used for vertical tillage. *Scientific Reports*, Vol. 11, 2537. https://doi.org/10.1038/s41598-021-82270-9
10. Aliiev, E., Tesliuk, H. (2024). Analytical justifications of constructive parameters of bionic colters for vertical soil treatment. *Machinery & Energetics*, Vol. 15(3), pp. 129–139. https://doi.org/10.31548/machinery/3.2024.129

11. Xu, G., Xie, Y., Peng, S., Liang, L., Ding, Q. (2023). Performance evaluation of vertical discs and disc coulters for conservation tillage in an intensive rice–wheat rotation system. *Agronomy*, Vol. 13(5), 1336. https://doi.org/10.3390/agronomy13051336
12. Ibrahmi, A., Bentaher, H. (2025). Simulation of tillage forces and soil movement during soil-disc plow interaction using FEM. *Scientific Reports*, Vol. 15, 36022. https://doi.org/10.1038/s41598-025-19961-0
13. Wu, P., Zhang, X., Chen, Y. (2025). Simulation of the micro-dynamics in soil–cornstalk–disc interactions using the discrete element method. *Smart Agricultural Technology*, Vol. 11, 100984. https://doi.org/10.1016/j.atech.2025.100984
14. Lopes, A.G.C., Filho, A.C.M., Santana, L.S., Martins, M.B., Silva, P.R.A., Franco, J.R., Da Silva Correia, T.P., Gomides, J.F.F.B. (2025). Effect of applied loads on passive rolling coulters for cutting crop residues. *Smart Agricultural Technology*, Vol. 10, 100702. https://doi.org/10.1016/j.atech.2024.100702
15. Badegaonkar, U.R., Kumar, M., Kamble, A.K., Thakare, S.H., Babu V.B., Kumar, M., Roul, A.K. (2025). Effect of powered disc coulters and residue holding wheel on cutting performance of rice residues under no-tillage system in soil bin. *Journal of Agricultural Science and Technology*, Vol. 27 (2), pp. 281–299. https://doi.org/10.22034/JAST.27.2.281
16. Badegaonkar, U.R., Kumar, M., Kamble, A.K., Thakare, S.H. (2024). Optimization of design parameters of press wheel attached straw cutting mechanism for rice residue in simulated field condition. *Journal of Scientific & Industrial Research*, Vol. 83(9), pp. 1033–1041.
17. Kamble, A.K., Thakare, S.H., Badegaonkar, U.R. (2018). Conservation agriculture: Crop residue cutting mechanisms for direct drilling in crop residual condition. *International Journal of Current Microbiology and Applied Sciences*, Vol. 6, pp. 379–387.
18. Wang, Q., Zhu, L., Li, M., Huang, D., Jia, H. (2018). Conservation agriculture using coulters: Effects of crop residue on working performance. *Sustainability*, Vol. 10(11), 4099. https://doi.org/10.3390/su10114099
19. Kozachenko, O., Aliiev, E., Sedykh, K. (2021). Results of investigation of the spring shank disc harrow performance. *UPB Scientific Bulletin, Series D: Mechanical Engineering*, Vol. 83(4), pp. 123–140.
20. Becker, R.S., Alonço, A.S., Francetto, T.R., Carpes, D.P., Zart, B.C.C.R., Moreira, A.R. (2019). Operational performance of crop residue cutting discs in the no-tillage system. *AgricEngInt: CIGR Journal*, Vol. 21(2), pp. 78–85.
21. Shevchenko, I.A. (2016). *Management of the Agrophysical State of the Soil Environment*. Vinichenko Publishing House. Kyiv, Ukraine.
22. Kobets, A., Aliiev, E., Tesliuk, H., Aliieva, O. (2023). Simulation of the interaction between the working bodies of tillage machines and the soil in Simcenter STAR-CCM+. *Machinery & Energetics*, Vol. 14(1), pp. 9–23. https://doi.org/10.31548/machinery/1.2023.09
23. Hutsol, O.P., Kovbasa, V.P. (2016). *Justification of the Parameters and Modes of Movement of Tillage Machines with Disc Working Bodies*. National University of Life and Environmental Sciences of Ukraine, Kyiv, Ukraine.
24. Aday, S.H. (2015). *Theory of Agricultural Machines*. Basrah University, Basrah, Iraq.
25. Ahmad, F., Khaliq, A., Qishuo, D., Chandio, F.A., Sultan, M., Awais, M. (2023). Energy-efficient tillage system for crop production. *In: A. Rakshit, A. Biswas, D. Sarkar, V.S. Meena, R. Datta (Eds.). Handbook of Energy Management in Agriculture*, pp. 501–525. Springer, Singapore. https://doi.org/10.1007/978-981-19-7736-7_26-1
26. Chang, C.-L., Ucgul, M. (2025). Innovative design and application of modern agricultural machinery systems in cropping systems. *Agriculture*, Vol. 15(22), 2371. https://doi.org/10.3390/agriculture15222371